

A Fast Anisotropic Mumford-Shah Functional Based Segmentation

J.F. Garamendi, N. Malpica, and E. Schiavi

Universidad Rey Juan Carlos, Móstoles, Madrid, Spain

{juanfrancisco.garamendi,norberto.malpica,emanuele.schiavi}@urjc.es

Abstract. Digital (binary) image segmentation is a critical step in most image processing protocols, especially in medical imaging where accurate and fast segmentation and classification are a challenging issue. In this paper we present a fast relaxation algorithm to minimize an anisotropic Mumford-Shah energy functional for piecewise constant approximation of corrupted data. The algorithm is tested with synthetic phantoms and some CT images of the abdomen. Our results are finally compared with manual segmentations in order to validate the proposed model.

1 Introduction

Image segmentation is a basic step in digital image analysis, and is especially important in the quantification of medical images. Classical segmentation methods include histogram based approaches as well as region and edge based detection. In recent years, active contour methods have become very popular, as they allow to embed both high and low level information into the segmentation process. The first models were curve evolution approaches to edge detection [1,2]. Recently, region based approaches such as the Active Contours without edges [3] have proved very useful in applications where the edges are not clearly defined. These models are normally resolved using level set curve evolution methods. The drawback is that they are normally very slow, which hinders their use in some applications where a fast segmentation is needed.

Fast numerical methods, such as the multigrid method, can be applied to these models [4]. Greater improvements can be obtained by finding equivalent models that allow faster numerical resolutions. Grady et al. reformulated the Mumford-Shah functional on an arbitrary graph and applied combinatorial optimization to produce a fast, low-energy solution [5]. In this paper, we propose a fast resolution of a weighted Mumford-Shah model for digital (binary) image segmentation by demonstrating its equivalence to a denoising model.

This paper is organized as follows: in Section 2 we briefly review the classical Rudin-Osher-Fatemi (ROF) denoising model [6] and the Chan-Vese Segmentation model [3], as well as the connection between them proposed by Chambolle [7]. Section 3 introduces the model problem, which is an anisotropic (weighted) version of the popular Mumford Shah model for piece-wise constant approximations, and the link between this model and the ROF model is established.

This links provides a new relaxation method which allows to solve numerically the segmentation problem in an efficient way. Numerical results are presented in section 4, and discussion and conclusion are presented in Section 5.

2 Material and Methods

2.1 The ROF Denoising Model

The ROF model is a variational method for image denoising which preserves the edges of the image, by regularizing only along (and not through) the image contours. Let $\Omega \subset \mathbb{R}^2$ be an open, bounded domain (usually a rectangle) where $(x, y) \in \Omega$ denotes pixel location. Image denoising is the process of reconstructing unknown data $u(x, y)$ from observed data $u_0(x, y)$, assuming that $u(x, y)$ has been corrupted by an additive noise $\eta(x, y)$, i.e. $u_0(x, y) = u(x, y) + \eta(x, y)$.

In [6], Rudin, Osher and Fatemi proposed to minimize the following energy functional

$$J(u) = \int_{\Omega} |\nabla u| dx dy + \frac{1}{2\lambda_{rof}} \int_{\Omega} (u - u_0)^2 dx dy \quad (1)$$

where λ_{rof} is a parameter which controls the trade off between the Total Variation term $\int_{\Omega} |\nabla u| dx dy$ (depending on the gradient of the reconstructed image u) and the data fidelity term. Small values of λ_{rof} indicates a strong belief on the data term u_0 while greater values provides strongly denoised versions of the reconstructed image u .

2.2 The Chan-Vese Segmentation Model

The Chan-Vese model for binary segmentation is based on the minimization of an energy functional expressed in terms of a level set formulation. For completeness, we briefly sketch the level set dictionary. Let $\omega \subset \Omega$ be an open, positive measured sub-region of the original domain (eventually not connected). If the curve C represents the boundary of such a segmentation ω then, in the level set formulation, the (free) moving boundary C is the zero level set of a Lipschitz function $\phi : \Omega \rightarrow \mathbb{R}$, that is: $C = \{(x, y) \in \Omega : \phi(x, y) = 0\}$, $C = \partial\omega$ where $\omega = \{(x, y) \in \Omega : \phi(x, y) > 0\}$, $\Omega \setminus \omega = \{(x, y) \in \Omega : \phi(x, y) < 0\}$. The level set function ϕ can be characterized as a minimum of the following energy functional:

$$E_{cv}(c_1, c_2, \phi) = \int_{\Omega} |\nabla H(\phi)| dx dy + \lambda_{cv} \int_{\Omega} H(\phi)(u_0 - c_1)^2 dx dy + \lambda_{cv} \int_{\Omega} (1 - H(\phi))(u_0 - c_2)^2 dx dy \quad (2)$$

where c_1 and c_2 represent the mean value inside and outside the segmented region and λ_{cv} is a weight factor which controls the length of the interface defining the two class segmentation. The function $H(x)$ represents the Heaviside function,

i.e.: $H(x) = 1$ if $x \geq 0$ and $H(x) = 0$ otherwise, and it allows to express the length of C by

$$|C| = \text{Length}(\phi = 0) = \int_{\Omega} |\nabla H(\phi)| dx dy.$$

2.3 The Link between Chan-Vese and ROF Model

The connection between the Chan-Vese segmentation model and the ROF denoising model was established by Chambolle [7]. Let us consider the minimization problem associated to (2) can be written in geometrical form:

$$\min_{E, c_1, c_2} J_{cv}(E, c_1, c_2)$$

where

$$J_{cv}(E, c_1, c_2) = P(E) + \frac{1}{2\lambda_{cv}} \left(\int_E (u_0 - c_1)^2 dx dy + \int_{CE} (u_0 - c_2)^2 dx dy \right)$$

and $P(E) = \int_{\Omega} |\nabla \chi_E| dx dy$ denotes (with abuse of notation) the perimeter of the set E and χ_E is the characteristic function of the set E . The proper formalism for $BV(\Omega)$ functions can be found in [8].

The key observation was that this minimization problem, embedded in a relaxation scheme, is equivalent to solving the ROF model and thresholding the solution obtained. This is based on the following result [7]:

Lemma 1. *Let u minimize the ROF energy (1) then, for any $s \in \mathbb{R}$, the set $E_s = \{u > s\}$ is a minimizer (over all sets $E \subset \Omega$) of*

$$J(E) = P(E) + \frac{1}{\lambda_{rof}} \int_E (s - f) dx dy$$

Once the λ parameter has been fixed, the relaxation scheme is as follows:

1. Fix an initial partition E^0 .
2. Minimize the energy $J_{cv}(E, c_1, c_2)$ w.r.t. the constants c_1 and c_2 , i.e. choose c_1 and c_2 like the mean inside E and CE respectively.
3. With c_1 and c_2 fixed by the previous step, minimize the energy $J_{cv}(E, c_1, c_2)$ w.r.t. the set E . This minimization problem has the same minima as [7]:

$$\min_E \left\{ P(E) + \frac{c_1 - c_2}{\lambda_{cv}} \int_E \left(\frac{c_1 + c_2}{2} - f \right) dx dy \right\}$$

By lemma 1, a solution E is given by $E_s = \{u > s\}$, where $s = (c_1 + c_2)/2$ and u minimizes the ROF energy:

$$\int_{\Omega} |\nabla u| dx dy + \frac{c_1 - c_2}{2\lambda_{cv}} \int_{\Omega} |u - f|^2 dx dy \quad (3)$$

4. Go to step 2 until convergence.

Notice that the iterative process generates a sequence of ROF problems with associated parameters $\{\lambda_{rof}^k\} = \{\lambda_{cv}/(c_2^{k-1} - c_1^{k-1})\}$, which have to be solved at each iteration. This is a drawback from the numerical point of view, as it slows down the final image segmentation. This introduces the main scope of our technique which is presented in the next section.

3 The Model Problem

3.1 Anisotropic Mumford-Shah Model

Osher and Vese proposed in [9] the following energy functional for image segmentation:

$$J_{ams}(E, c_1, c_2) = |c_2 - c_1|P(E) + \frac{1}{2\lambda} \left(\int_E (u_0 - c_1)^2 dx dy + \int_{cE} (u_0 - c_2)^2 dx dy \right) \quad (4)$$

This energy functional is a modified version of the original Chan-Vese active contours without edges model (2), and represents an anisotropic version of the Mumford-Shah Energy functional, for piecewise constant approximations [10]. If we compare both functionals, (2) and (4), we can notice that the length term $P(E)$ is weighted by the jump $|c_2 - c_1|$. When both models are solved with the same λ parameter, the anisotropic model provides a more detailed segmentation and finer scales are resolved (see figure 2).

3.2 The Link between the Anisotropic Mumford-Shah Model and ROF Model

Our proposal is to apply Chambolle's result described in section 2.3 to the functional (4). This leads to a relaxation scheme in which it suffices to solve the ROF model just once, thus allowing a notable speed-up of the final segmentation.

The presented relaxation scheme is as follows:

1. Initialize c_1 and c_2 .
2. Fixed c_1 and c_2 by the previous step, minimize the energy $J_{ams}(E, c_1, c_2)$ w.r.t. the set E . Assume $c_i > c_j$, $i = 1, 2$, $j = 1, 2$, $i \neq j$. It can be shown that this minimization problem has the same minima as:

$$\min_E \left\{ |c_i - c_j|P(E) + \frac{c_i - c_j}{\lambda} \int_E \left(\frac{c_i + c_j}{2} - f \right) dx dy \right\} \quad (5)$$

The term $|c_i - c_j|$ can be factorized and as result, the minimization problem (5) has the same minima as:

$$\min_E \left\{ P(E) + \frac{1}{\lambda} \int_E \left(\frac{c_i + c_j}{2} - f \right) dx dy \right\} \quad (6)$$

According to lemma 1 showed in section 2.3, a solution E is given by $E_s = \{u > s\}$, where $s = (c_1 + c_2)/2$ is the threshold and u minimizes the ROF energy (1).

3. With E fixed by the previous threshold step, minimize the energy $J_{ams}(E, c_1, c_2)$ w.r.t the constants c_1 and c_2 . The minimization leads to the following expressions

$$c_1 = \bar{u}_0^E - \lambda \frac{c_1 - c_2}{|c_1 - c_2|} \frac{P(E)}{|E|} \quad c_2 = \bar{u}_0^{CE} - \lambda \frac{c_2 - c_1}{|c_1 - c_2|} \frac{P(CE)}{|CE|} \quad (7)$$

where \bar{u}_0^E and \bar{u}_0^{CE} are the local averages of the image u_0 on the corresponding regions, and $|E|$, $|CE|$ are the area enclosed by the regions E and CE .

4. Go to step 2. until stabilization.

Notice that in this iterative process there is only one ROF problem to minimize. The minimum is attained solving the associated elliptic Euler-Lagrange equation with multigrid methods [11].

4 Numerical Results

The relaxation algorithm proposed has been tested on synthetic images with geometrical figures (see figure 1), as well as on medical images with the aim of segmenting the liver in Computerized Tomography (CT) images. In all cases the elliptic Euler-Lagrange equation has been solved following a multigrid scheme [11,12] with maximum final residual below $9 \cdot 10^{-3}$ in the experiments. The multigrid used is composed of a F cycle with 2 and 3 pre and post smoothing iterations respectively. The smoother is a non-linear Gauss-Seidel line-wise ω -relaxation with $\omega = 1.3$. The transfers operators are full-weighting for fine-to-coarse interpolation of the residual, injection for fine-to-coarse interpolation of the solution and linear interpolation for coarse-to-fine interpolation of the error.

We first compared the two models, the Chan-Vese and Anisotropic Mumford-Shah Models. The results, in figure 2, show that for the same value of λ , the anisotropic Mumford-Shah model produces a more detailed segmentation, but similar results can be obtained with a correctly chosen λ value.

Figure 3 shows the segmentation over the synthetic images. The values of the parameter λ has been set to $\lambda = 0.3$, $\lambda = 0.5$, $\lambda = 1$ and $\lambda = 2$, notice that as in Chan-Vese model, larger values produce a smoother segmentation, .

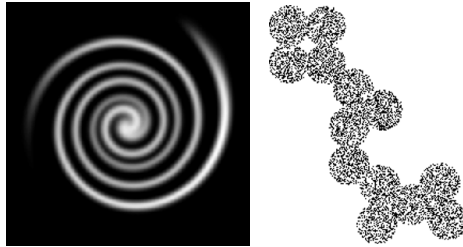


Fig. 1. The synthetic spiral and circles images used on the algorithm tests

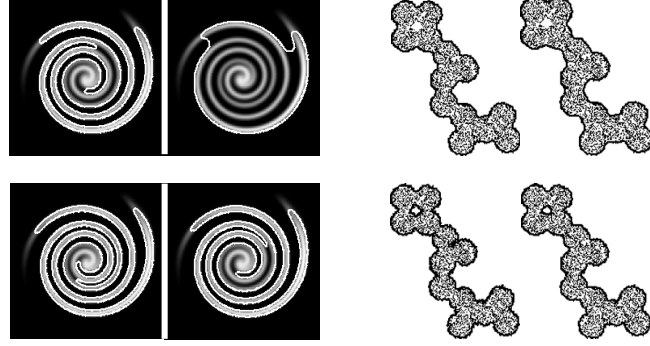


Fig. 2. Comparison between the models of Chan-Vese (first row) and Anisotropic Mumford Shah (second row) solved respectively with Chambolle's relaxation and our proposal. The values of λ are 0.3 for first and third columns and 0.5 for second and four columns.

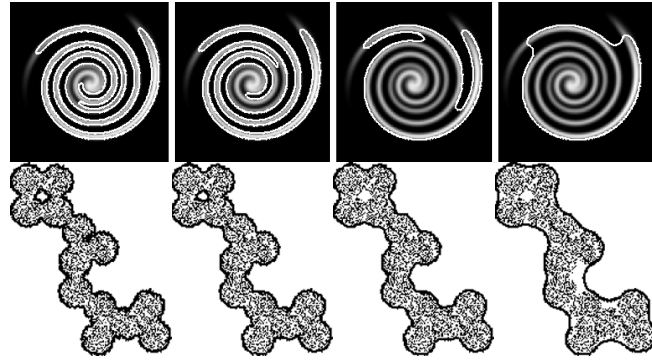


Fig. 3. Effect of λ parameter over spiral and circles images, from left to right the values of λ used has been 0.3, 0.5, 1 and 2

The algorithm has also been tested on several CT data sets series acquired at Fundación Hospital Universitario de Alcorcón, in Madrid (Spain) to segment the liver. The validity of the Chan-Vese and anisotropic Mumford-Shah models to segment the liver in CT images has been previously shown in [13] and [12] respectively. The CT images used were acquired in a General Electric LightSpeed CT scanner. The data sets size is $512 \times 512 \times 40$ with spatial resolution of 0.74×0.74 mm and with a slice thickness of 5 mm. The automatic liver segmentation has been compared against manually segmented images from an expert radiologist. We use the commercial software Mimics (TM) by Materialise Software to produce a manual segmentation of the liver. Also we loaded the automatic segmentation provided by our method to produce a visual comparative between both segmentations. Figure 4 shows three slices from one data sets and a 3D reconstruction of the automatic segmentation, where the differences between a manual

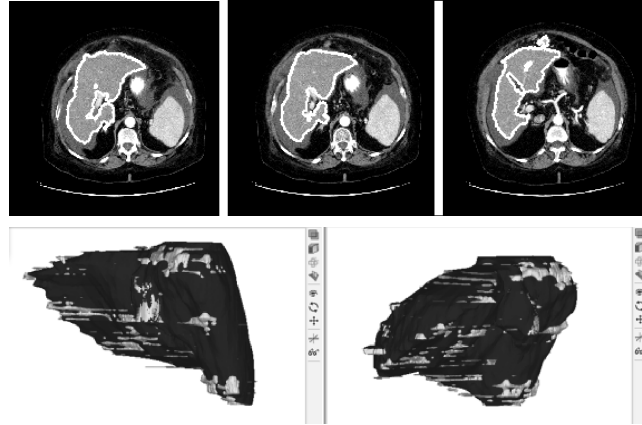


Fig. 4. Automatic liver segmentation done with the proposal method. In the first row, 2D axial views of three slices are shown, and in the second row, two different views from 3D segmentation loaded in Mimics, where dark color shows the automatic segmentation and light color shows the error with respect manual segmentation.

segmentation are marked in lighter color. It can be shown that the relaxation algorithm works well in most slices, but there are some slices with a significant error, this is consequence that the relaxation scheme can be get trapped in a local minimum. This occurs with both relaxation models described in sections 2.3 and 3.2.

5 Discussion and Further Work

In this paper we have presented a novel method for fast (binary) digital image segmentation. It is based on a previous method by Chambolle that uses a relaxation scheme in which the ROF equation is solved several times. Our method requires solving the ROF model only once. The preliminary numerical results over synthetic images are promising from both the quantitative and qualitative point of view. In this case, the method works well and finer structures can be recovered tuning the λ parameter. When medical segmentation applications are considered relaxation scheme can converge to a local minimum. The main difference between manual and automatic liver segmentations lies in blood vessels which are wrongly included by our method.

In the way towards fully automatic liver segmentation, future work will address the above problem following the previous results in [12] where manual selection of the best threshold showed more accurate liver segmentation.

Acknowledgements

This work was partially supported by projects LAIMBIO - PRICIT 05/05 , financed by Comunidad de Madrid, MTM2005-03463 and CCG07-UCM/ESP-2787.

References

1. Kass, M., Witkin, A., Terzopoulos, D.: Snakes: Active Contour Models. *International Journal of Computer Vision* 1(4), 321–331 (1988)
2. Caselles, V., Catté, F., Coll, B., Dibos, F.: A geometric Model for Active Contours in Image Processing
3. Chan, T.F., Vese, L.A.: Active Contours Without Edges. *IEEE Transactions on Image Processing* 10(2), 266–277 (2001)
4. Badshah, N., Chen, K.: Multigrid method for the Chan-Vese model in variational segmentation. *Commun. Comput. Phys.* 4, 294–316 (2008)
5. Grady, L., Alvino, C.: Reformulating and optimizing the Mumford-Shah functional on a graph - A faster, lower energy solution. In: Forsyth, D., Torr, P., Zisserman, A. (eds.) *ECCV 2008, Part I. LNCS*, vol. 5302, pp. 248–261. Springer, Heidelberg (2008)
6. Rudin, L.I., Osher, S., Fatemi, E.: Nonlinear total variation based noise removal algorithms. *Physica D* 60, 259–268 (1992)
7. Chambolle, A.: An Algorithm for Total Variation Minimization and Applications. *Journal of Mathematical Imaging and Vision* 20(1-2), 89–97 (2004)
8. Ambrosio, L., Fusco, N., Pallara, D.: Functions of bounded variation and free discontinuity problems. In: *Oxford Mathematical Monographs*, pp. xviii+434. The Clarendon Press/ Oxford University Press, New York (2000)
9. Osher, S., Paragios, N.: *Geometric Level Set Methods in Imaging, Vision, and Graphics*. Springer, Heidelberg (2003)
10. Mumford, D., Shah, J.: Optimal approximations by piecewise smooth functions and associated variational problems. *Commun. Pure Appl. Math.* 42, 577–685 (1989)
11. Trottenberg, U., Oosterlee, C., Schüller, A.: *Multigrid*. Academic Press, London (2001)
12. Garamendi, J.F., Malpica, N., Schiavi, E., Gaspar, F.J.: ROF based segmentation of the liver in ct images. In: *Congreso Anual de la Sociedad Española de Ingeniería Biomedica* (2008)
13. Garamendi, J.F., Malpica, N., Martel, J., Schiavi, E.: Automatic Segmentation of the Liver in CT Using Level Sets Without Edges. In: Martí, J., Benedí, J.M., Mendonça, A.M., Serrat, J. (eds.) *IbPRIA 2007. LNCS*, vol. 4477, pp. 161–168. Springer, Heidelberg (2007)